MODELLING CONVERTED WAVES FOR SUB-BASALTIC IMAGING

Peter Hanßen[1,2] and Xiang-Yang Li[1]

[1] British Geological Survey, West Mains Road, Edinburgh
[2] Department of Geology and Geophysics, University of Edinburgh

SUMMARY

Due to the high seismic velocities of elastic waves in basalts the energy of an incident P-wave in a seismic reflection profile is mostly reflected. Standard seismic processing is not able to produce an image of any structure beneath such basaltic layers. Furthermore in offshore measurements, numerous multiple reverberations between the sea surface and the sea floor, and between the sea surface and the top-basalt interface, hide weak responses of any sub-basaltic layers. Here, to gain information about these sub-basaltic reflectors we investigate the mode conversions using full-wave modelling. The conversions may occur at both the top and the bottom of the basaltic layer. The resulting converted shear waves transport more energy through the high-velocity layer on their way down and up, especially if the shear wave velocity inside the layer is close to the P-wave velocities of the surrounding rocks. The converted wave with only S-modes through the basalt shows the strongest amplitude for the models studied. The converted wave with only S-modes below the top of the basalt is the second strongest, and shows almost continuous amplitude and phase over a long offset. Due to the interference of multiples and converted shear waves in the near-offset range, the profile length in offshore recordings has to be longer than the commonly used 4 to 6 km.

INTRODUCTION

In the Northeast Atlantic Margin a major problem for hydrocarbon exploration is the wide occurrence of basaltic layers (Hitchen and Stoker, 1995). Over recent years, considerable efforts and resources have been focused on improving seismic imaging beneath basalt. New acquisition techniques for this purpose include two-boat shooting (Emsley, 1997, Frühn et al., 1998) and seabed seismic (Samson et al., 1995). P The use of converted waves for sub-basaltic imaging, in particular, has attracted considerable interest (for example Li et al., 1997 and 1998, Gulati and Stewart, 1997, Longshaw, 1998). Despite all these efforts, there is a general lack of understanding in the fundamental behaviour of the converted wave and their possible interference with multiples, and refracted waves. This has not only implications on data processing, but also in acquisition design and cost-effectiveness analysis. Based on numerical calculations of reflection amplitude in layered media and full-wave modelling, we investigate and compare different types of conversions and assess their feasibilities for sub-basaltic imaging.

AMPLITUDE BEHAVIOUR

To verify which wave type will give the best response of sub-basaltic interfaces, we calculated the effective reflection and transmission coefficients for a horizontally layered and isotropic model from the Rockall area (Li et al., 1998). This ideal model (Figure 1) consists of two sandstone units overlaid by a basaltic layer, which is itself overlaid by a sediment unit and the water column. The shear-wave velocity, v_S, of the basalt is close or equal to the primary-wave velocity, v_P, of the surrounding rocks. This leads to high conversion coefficients at the top and the bottom interface of the basalt.

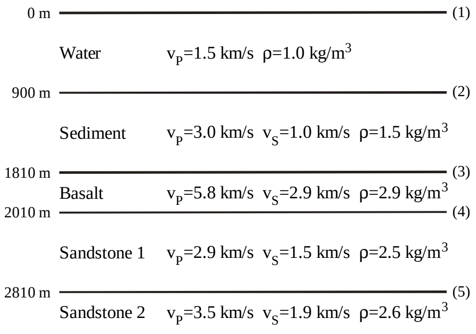

Figure 1: Rockall model.

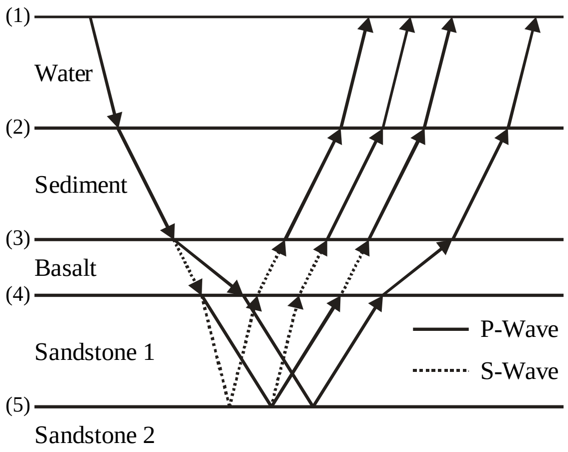

Figure 2: Rays for three converted waves and the pure P-wave travelling from the sea surface to interface 5, and back, for the Rockall model.

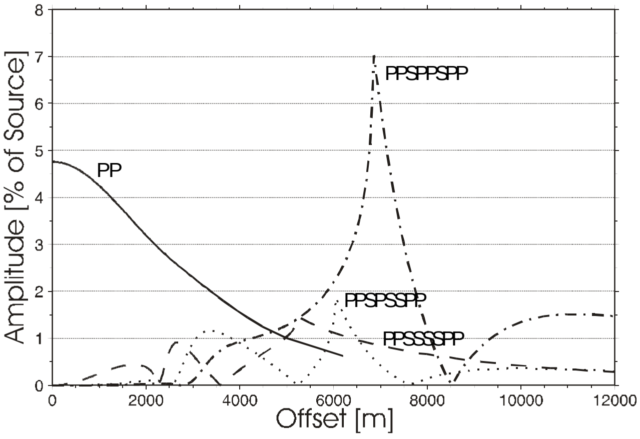

Figure 3: Effective reflection coefficients for the ideal Rockall model and for the waves shown in Figure 2.

We address two different converted wave modes proposed by Purnell et al. (1990) and Gulati and Steward (1997): PPSPPSPP and PPSPSSPP. They travel from the sea surface to interface 5 and back (Figure 2). We also examine the behaviour of the PP-wave, which only travels as P-waves to the interface and back, and a type of converted wave reported by Emsley et al. (1997) in real data: PPSSSSPP. Figure 3 shows the resulting effective reflection coefficients calculated using Aki and Richards (1980). The coefficients are normalised by the source amplitude. The P-wave (PP) gets refracted just beyond 6 km offset, while in contrast the locally converted S-waves is detectable up to 12 km. Furthermore it can be seen that the PPSPPSPP-wave with S-waves only inside the basalt has the highest amplitude at offsets around 7 km. The amplitude is about 7 % of the source amplitude and the second strongest converted wave is only 1.9 %. All amplitudes in the following figures are plotted with their absolute values for a better comparison between different wavetypes. A change in sign of a wave occurs when a curve touches the zero amplitude value. This is the case for PPSPPSPP but does not happen as frequently for PPSSSSPP, which consists of only S-waves below the top of the basalt. Therefore this wave could be consistently detectable for the whole offset, despite the fact that the amplitude is at least two times smaller than that of PPSPPSPP.

The calculations show that sufficient high amplitudes of reflections from below high-velocity basalt layers for locally converted S-waves can be expected. This is most prominent if the S-wave velocity of the basalt matches the P-wave velocity of the surrounding layers above and below. The strongest wave is the mode with S-waves on the way down and up only in the basalt (PPSPPSPP). The second strongest mode is the one with only S-waves below the top of the basalt (PPSSSSPP) with an additional benefit of an almost constant amplitude over most far offsets. The wave with an asymmetrical ray path (PPSPSSPP) is of lowest amplitude and may only be observed in special cases like an inhomogeneous layering (Gulati and Stewart, 1997).

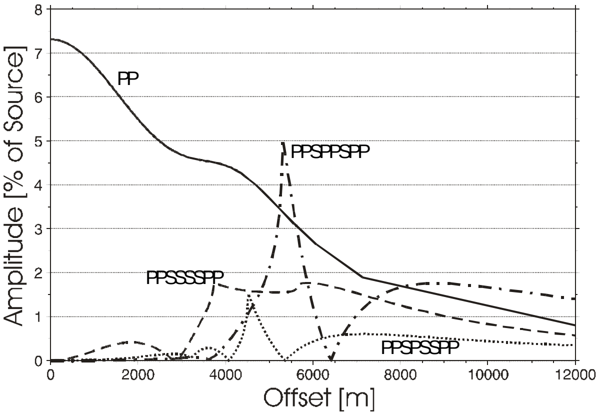

Figure 4: Effective reflection coefficients for the non-ideal Rockall model.

Figure 4 shows the effective reflection coefficients for another model. In this non-ideal model the sediment overlaying the basalt (see Figure 1) is split into two different layers:

- Sediment 1 at 900m depth:
  v_P=1.7 km/s, v_S=0.6 km/s, ρ=2.1 kg/m^3.
- Sediment 2 at 1160m depth:
  v_P=2.6 km/s, v_S=0.9 km/s, ρ=2.2 kg/m^3.

Additionally we reduced the velocities in these sedimentary layers to increase the contrast with the underlying basalt. This results in an increase of the PP-wave at near-offsets and a decrease of the PPSPPSPP-amplitude when compared to the ideal-model calculations shown in Figure 3. The non-ideal model shows, that the PP-wave is present throughout the 12 km offset and additionally, that the wave with only S-waves through the basalt has the highest amplitude from 8 km onwards.

MODELLING STUDIES

To verify these calculations we calculated synthetic seismograms of the two Rockall model using the OSIRIS modelling package. Figure 5 shows the recordings of 30 receivers up to 6 km offset for the first 6 seconds. The source is at zero-offset at 10 m water depth and the receivers are at 15 m water depth with an initial offset and interval of 200 m.

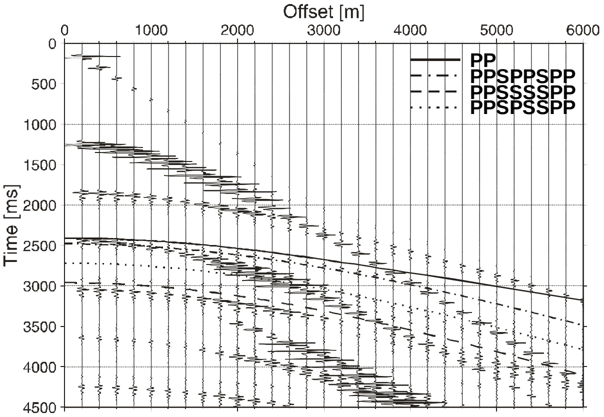

Figure 5: Near-offset synthetic seismogram for the ideal Rockall model with overlaying reflection traveltime curves of interface 5.

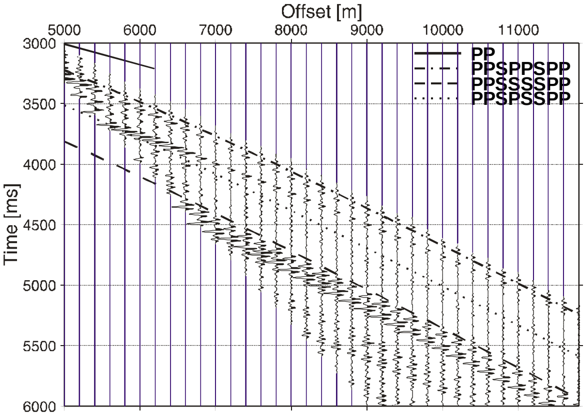

Figure 6: Far-offset wavetrain of a synthetic seismogram for the ideal Rockall model with overlaying reflection traveltime curves of interface 5.

Strong multiples are observed at near offsets. The water multiple completely masks a possible detection of the PP reflection. Additionally we find strong reverberations caused by the basalt top which disturb the image at near offset.

This means that an extension beyond 6 km offset is necessary. Also to focus on the maximum amplitude of the PPSPPSPP-mode, we extended the offset to 12 km. At this range all target events run in between the sea bottom and the basalt top reflection, which form a far-offset wavetrain, as identified by Li et al. (1998). In Figure 6 we muted the PP-reflection of the seabed to enlarge the amplitudes inside the wavetrain and cut off the near-offset. We still have multiples in this area, reflections of other interfaces and additionally refracted waves. The PPSPPSPP-wave can be tracked up to 10 km and does not appear to be affected by the amplitudes of the refracted waves. The sediment multiple has a smaller amplitude than the PPSPPSPP-mode and has a large enough time difference to be effective. The PPSPSSPP-wave with its asymmetric ray path is hardly detectable around 7 km but we have a strong first break of the PPSSSSPP-wave without any disturbances.

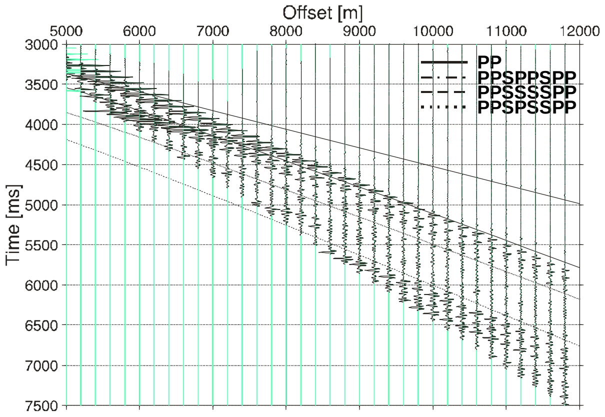

Figure 7: Far-offset wavetrain of a synthetic seismogram for the non-ideal Rockall model with overlaying reflection traveltimes from interface 5.

The far-offset wavetrain shown in Figure 7 is calculated for the non-ideal model. The PP-mode gets refracted at a greater offset than the ideal model and its amplitude is the highest of all calculated waves from the target. At far-offsets the PPSPPSPP-wave has the highest amplitude as shown in Figure 4. In this non-ideal case the top-basalt reflection and additional multiples cover the converted wave arrivals. The amplitudes of these waves are so high that additional crossings of refracted and reflected modes are negligible. The reflected target events with only P-modes is the second strongest response at far-offsets but cannot be traced even in the most undisturbed area of the seismogram. The amplitudes of the two other converted target waves are less than the PP-wave and will be negligible.

DISCUSSIONS AND CONCLUSION

The calculation of effective reflection coefficients for a model with interbedded basalt shows that the amplitudes of converted waves can be sufficient for imaging below high-velocity layers. Of these, the wave with S-modes only through the basalt is the one with the strongest amplitude. Because the maximum amplitude of this wave occurs at an offset beyond 6 km and the near-offset is highly disturbed by multiples, which hamper the recognition of the P-wave, an acquisition should include these far-offset ranges. Additionally the converted wave with only S-modes below the top of the basalt shows almost continuous amplitude and phase over a long offset and this feature may be useful in real data analysis. Waves with an asymmetrical ray path like the PPSPSSPP-mode can be neglected, because of their weak amplitudes and occasional phase shifts. Unfortunately there are multiples in addition to the usual water reverberations, which not only disturb the near-offset but also in certain extend the far-offset target events. At these far-offsets we also have to deal with different crossing reflections and refractions.

ACKNOWLEDGEMENTS

Peter Hanßen and Xiang-Yang Li are funded by the sponsors of the Edinburgh Anisotropy Project. We thank Colin MacBeth and Anton Ziolkowski for their comments on this work. This work is published with approval of the Director of the British Geological Survey and the EAP sponsors: Agip, Amerada Hess, BP-Amoco, BG plc, Chevron, Elf, Fina, Mobil, PGS, Phillips, Saga Petroleum, Schlumberger, Shell, Texaco and Veritas DGC.

REFERENCES

Aki, K. and Richards, P. G., 1980. *Quantitative Seismology - Theory and Methods*. W. H. Freeman and Company.

Emsley, D., Davis, P. and Boswell, P., 1997. A Sub-Basalt Imaging Experiment, West of Hebrides 1996. CMPT Sub-Basalt Imaging Workshop, Barbican Centre, London, October 1997.

Frühn, J., White, R. S., Fliedner, M., Richardson, K. R., Cullen, E., Latkiewicz, C., Kirk, W. and Smallwood, J. R., 1997. Two-ship large aperature seismic profiles - application to imaging through basalt. 60th EAGE Leibzig, Extended Abstracts, 1-47

Gulati, J. S. and Stewart, R. R., 1997. Seismic exploration through high-velocity layers. 67th Annual Internat. Mtg., Soc. Expl. Geophys., Expanded Abstracts, p. 1297-1300.

Hitchen, K. and Stoker, M., 1995. The Rockall Continental Margin – A potential petroleum province. Earthwise, British Geological Survey, 7, 26-27.

Li, X.-Y. and MacBeth, C., 1997. Imaging beneath basalt using converted waves in marine seismic data. 57th EAGE Geneva, Extended Abstracts, Vol. 1, A038.

Li, X.-Y. and MacBeth, C. and Hitchen, K. and Hanßen, P., 1998. Using converted shear-waves for imaging beneath basalt in deep water plays. 68th Annual Internat. Mtg., Soc. Expl. Geophys., Expanded Abstracts, Vol. 2, p. 1369-1372.

Longshaw, S. K., Sunderland, J. and Horn, I., 1998. Mode Conversion and Multiples. 68th Annual Internat. Mtg., Soc. Expl. Geophys., Expanded Abstracts, Vol. 2, p. 1340-1342.

Purnell, Guy W. and McDonald, J. A. and Sekharan, K. K. and Gardner, G. H. F., 1990. Imaging beneath a High-Velocity Layer Using Converted Waves. 60th Annual Internat. Mtg., Soc. Expl. Geophys., Expanded Abstracts, p. 752-755.

Samson, C., Barton, P. J. and Karwatowski, J., 1995. Imaging beneath an opaque basaltic layer using densely sampled wide-angle OBS data. Geophysical Prospecting 43, p. 509-527.